Research Square

Preprints are preliminary reports that have not undergone peer review.
They should not be considered conclusive, used to inform clinical practice,
or referenced by the media as validated information.

Spread through air spaces in lung adenocarcinoma with subsequent contralateral metachronous pulmonary lesion: a case report

Lulu Gao
Department of Radiology, Zhejiang Hospital
Bin Lin
zjdxlinbin@zju.edu.cn

Department of Radiology, the Second Affiliated Hospital, Zhejiang University School of Medicine

Case Report

Keywords: Spread through air spaces (STAS), Lung adenocarcinoma, Cinematic rendering, Metachronous pulmonary lesion, EGFR T790M, Almonertinib, Case report

Posted Date: September 27th, 2026

DOI: https://doi.org/10.21203/rs.3.rs-10794101/v1

License: This work is licensed under a Creative Commons Attribution 4.0 International License.
Read Full License

Additional Declarations: No competing interests reported.

Abstract

Background

Spread through air spaces (STAS) is a pattern of invasion in lung adenocarcinoma introduced by the World Health Organization in 2015. STAS is associated with increased recurrence risk and reduced survival. Herein, we report a case of lung adenocarcinoma with STAS in which cinematic rendering provided intuitive three-dimensional visualization of satellite nodules, followed by a contralateral pulmonary lesion 18 months later harboring a de novo EGFR T790M/L858R double mutation, managed with surgery and adjuvant almonertinib.

Case presentation

A 53-year-old Chinese woman had a pulmonary mass incidentally discovered on chest CT during a routine medical examination. Chest CT revealed a 2.8 cm mass in the left lower lobe with multiple peritumoral satellite nodules. Cinematic rendering reconstruction clearly depicted the satellite nodules and their spatial relationship with adjacent structures. The patient underwent video-assisted thoracoscopic surgery (VATS) left lower lobectomy with mediastinal lymph node dissection. Postoperative pathology confirmed invasive lung adenocarcinoma (acinar predominant, with papillary [20%], micropapillary [15%], and focal poorly differentiated [5%] components) with STAS, pathological stage pT1cN0cM0 (AJCC 9th edition). No adjuvant therapy was administered. Follow-up chest CT every 6 months revealed a new 0.6 cm nodule in the right middle lobe 18 months postoperatively. The patient underwent VATS right middle lobectomy with mediastinal lymph node dissection. Pathology confirmed a second invasive lung adenocarcinoma (acinar 40%, papillary 40%, micropapillary 20%, grade 3), stage pT1aN0cM0. Genetic testing revealed EGFR T790M (exon 20) and L858R (exon 21) double mutation. The patient was started on adjuvant almonertinib (110 mg daily) and remained recurrence-free at 20 months of almonertinib therapy.

Conclusions

This case demonstrates that peritumoral satellite nodules on CT reliably indicate STAS, and STAS-positive patients require vigilant surveillance for metachronous pulmonary lesions. Cinematic rendering provides intuitive visualization of STAS-related satellite nodules, aiding surgical planning. The de novo EGFR T790M/L858R double mutation in the metachronous lesion raises important considerations regarding tumor clonality, possible germline EGFR T790M, and the role of third-generation EGFR-TKIs as adjuvant therapy.

Background

Lung cancer remains the leading cause of cancer-related mortality worldwide, with lung adenocarcinoma being the most common histological subtype [1]. Despite advances in early detection through low-dose computed tomography (CT) screening and improvements in surgical techniques, a subset of early-stage lung adenocarcinoma patients still experience recurrence and metachronous tumors following curative-intent resection [2]. The identification of reliable prognostic markers is therefore essential for optimizing treatment strategies and surveillance protocols.

In 2015, the World Health Organization (WHO) classification of lung tumors introduced the concept of spread through air spaces (STAS) as a novel pattern of invasion in lung adenocarcinoma [3]. STAS is defined as the presence of micropapillary clusters, solid nests, or single tumor cells within air spaces in the lung parenchyma beyond the edge of the main tumor. This concept was further refined in the 2021 WHO classification, which established STAS as the fourth mode of tumor invasion, alongside stromal, vascular, and pleural invasion [4]. The presence of STAS excludes a diagnosis of adenocarcinoma in situ or minimally invasive adenocarcinoma, thereby upstaging the tumor and influencing therapeutic decisions.

The incidence of STAS in lung adenocarcinoma ranges from 14.8% to 60.5%, depending on the study population, pathological assessment methods, and classification criteria [5, 6]. STAS has been strongly associated with nodal and distant metastasis, advanced tumor stage, high-grade histological patterns (particularly micropapillary and solid predominant subtypes), lymphovascular invasion, and reduced survival outcomes [5, 7, 8]. Moreover, STAS is an independent risk factor for tumor recurrence, especially in patients undergoing limited (sublobar) resection [7, 8]. Notably, STAS has been identified as a risk factor for pulmonary metastasis after surgery [20].

The prognostic significance of STAS has important surgical implications. Multiple studies and meta-analyses have demonstrated that STAS-positive patients who undergo sublobar resection have significantly worse recurrence-free survival (RFS) and overall survival (OS) compared to those who undergo lobectomy [8, 9, 10]. A recent meta-analysis by Xu et al. confirmed that lobectomy provides additional survival benefits to STAS-positive patients compared with sublobar resection (RFS: hazard ratio [HR] = 1.97; OS: HR = 1.91) [10]. Consequently, preoperative identification of STAS has become critical for surgical planning.

Several CT morphological features have been identified as potential predictors of STAS, including larger tumor diameter, higher consolidation-to-tumor ratio (CTR), solid nodule type, pleural indentation, lobulation, spiculation, and the presence of peritumoral satellite nodules [11, 12, 13]. Among these, peritumoral satellite nodules represent a highly reliable imaging indicator of STAS, as they directly reflect the aerogenous spread of tumor cells beyond the main tumor margin [11]. Cinematic rendering is a recently developed photorealistic three-dimensional (3D) visualization technique that utilizes a complex global lighting model to generate lifelike images from standard volumetric CT data, providing superior depth perception and anatomical detail compared with conventional volume-rendering techniques [14, 15, 16].

The molecular landscape of STAS-positive tumors has been investigated, with studies showing that STAS is more frequently observed in tumors with wild-type EGFR, although STAS can also occur in EGFR-mutant tumors [21]. The relationship between STAS and EGFR mutation status, as well as the implications for targeted therapy, remains an active area of investigation. Epidermal growth factor receptor (EGFR) mutations, particularly exon 19 deletions and the L858R point mutation in exon 21, are the most common actionable driver mutations in lung adenocarcinoma, especially in Asian, female, never-smoker populations [25]. The T790M mutation in exon 20 is most commonly acquired as a resistance mechanism following treatment with first- or second-generation EGFR tyrosine kinase inhibitors (TKIs), but de novo T790M mutations (detected before TKI treatment) are rare, occurring in less than 1% of all lung cancers and approximately 2% of EGFR-mutant lung cancers [25, 26]. Approximately 50% of de novo T790M mutations are of germline origin, and about 73% of germline T790M carriers have a concomitant somatic EGFR-activating mutation, most commonly L858R [25, 26, 27].

Third-generation EGFR-TKIs, including almonertinib (aumolertinib, HS-10296), were specifically designed to inhibit both sensitizing EGFR mutations and the T790M resistance mutation. Almonertinib, the first domestically developed third-generation EGFR-TKI in China, has demonstrated potent inhibitory activity against T790M, T790M/L858R, and T790M/del19 (IC50: 0.37, 0.29, and 0.21 nM, respectively) [28]. In the phase III AENEAS trial, almonertinib significantly prolonged median progression-free survival to 19.3 months compared with 9.9 months for gefitinib in patients with advanced EGFR-mutant NSCLC [29]. The use of almonertinib in the adjuvant setting for resected EGFR-mutant NSCLC is currently being investigated in clinical trials [30].

In this case report, we present a patient with lung adenocarcinoma with STAS in whom cinematic rendering provided intuitive 3D visualization of STAS-related satellite nodules. Eighteen months after the initial surgery, a contralateral pulmonary lesion was detected and resected, revealing a second invasive lung adenocarcinoma harboring a de novo EGFR T790M/L858R double mutation. We review the current literature on STAS, metachronous pulmonary lesions, de novo EGFR T790M mutations, and the role of third-generation EGFR-TKIs in the adjuvant setting.

Case presentation

A 53-year-old Chinese woman was found to have a pulmonary mass incidentally on a chest CT during a routine medical examination 5 months prior to presentation. She exhibited no symptoms of cough, sputum production, hemoptysis, chest tightness, dyspnea, fatigue, night sweats, or chest discomfort. She had no history of smoking, occupational exposure to carcinogens, or previous pulmonary diseases. Her family history was unremarkable for malignancy.

Upon hospitalization, a thorough physical examination revealed no abnormalities. The respiratory sounds of both lungs were clear, with no audible dry or wet rales. No clubbing of fingers or supraclavicular lymphadenopathy was detected. Laboratory test results, including complete blood count,

liver and kidney function tests, electrolytes, blood glucose, and coagulation profile, were all within normal ranges. Tumor markers, including carcinoembryonic antigen (CEA), cytokeratin-19 fragment (CYFRA21-1), and squamous cell carcinoma antigen (SCC), were within normal limits.

Chest CT examination (Fig. 1A and B) revealed a mass lesion measuring approximately 2.8 cm in the superior segment of the left lower lobe. The mass showed traction adjacent to the visceral pleura, with pleural indentation. The lesion presented with lobulation and spiculation, and its density was heterogeneous, with a solid component predominating. Multiple small satellite nodules were observed surrounding the main lesion, located within 2 cm of the tumor margin, measuring 2–5 mm in diameter. No calcification, cavitation, or fat density was identified within the lesion. No mediastinal or hilar lymphadenopathy was observed. No pleural effusion or pericardial effusion was present.

The cinematic rendering reconstruction technique (Fig. 1C–F) was applied using a syngo.via post-processing workstation (Siemens Healthineers, Erlangen, Germany) with different color templates. The cinematically rendered images clearly depicted the metastatic small solid nodules surrounding the main lesion, which appeared as distinct satellite foci separate from the primary tumor mass. Different color templates highlighted different anatomical structures: one template emphasized the pulmonary vasculature and its relationship to the tumor, while another template clearly showed the relationship of the lesion with the bronchus and lung parenchyma. The 3D visualization provided superior depth perception and spatial relationship assessment compared with conventional axial and coronal CT images.

Based on the imaging findings, particularly the presence of peritumoral satellite nodules, clinical suspicion for lung adenocarcinoma with STAS was raised. The patient underwent preoperative evaluation, including pulmonary function tests and cardiac assessment, which revealed no contraindications to surgery. Given the concern for STAS based on imaging findings, lobectomy rather than sublobar resection was recommended to ensure adequate surgical margins.

The patient underwent video-assisted thoracoscopic surgery (VATS) left lower lobe lobectomy with systematic mediastinal lymph node dissection. Intraoperative findings confirmed a firm mass in the superior segment of the left lower lobe, with pleural retraction. The tumor was completely resected with negative surgical margins.

Postoperative histological examination confirmed the diagnosis of invasive lung adenocarcinoma, measuring 3.0 × 2.5 cm. The histological subtypes were acinar predominant, with papillary (approximately 20%), micropapillary (approximately 15%), and focal poorly differentiated (approximately 5%) components. Tumor cell clusters were identified spreading into the alveolar spaces beyond the main tumor margin, consistent with STAS. No lymphovascular invasion or visceral pleural invasion was identified. The bronchial resection margin was negative. Immunohistochemical examination showed: PD-L1 (E1L3N) negative; CD10 (focal positive); CD31, CD34, CD105, SMA, and CD163 positive. All resected lymph nodes were negative for metastasis. The pathological stage was pT1cN0cM0 (AJCC 9th edition, Stage IA3).

The patient made an uneventful postoperative recovery and was discharged on postoperative day 5. Given the stage IA3 disease with negative lymph nodes and negative margins, no adjuvant chemotherapy or targeted therapy was administered. The patient was followed up with chest CT every 6 months.

Eighteen months after the initial surgery, follow-up chest CT revealed a new nodule measuring 0.6 cm in the right middle lobe, which was highly suspicious for malignancy (Fig. 2). The nodule was a solid lesion with regular margins. No other new pulmonary nodules, mediastinal lymphadenopathy, or distant metastases were identified on staging evaluation, including brain MRI and abdominal CT. Given the suspicious imaging features and the patient's prior history of lung adenocarcinoma with STAS, surgical resection was recommended.

The patient underwent VATS right middle lobe lobectomy with mediastinal lymph node dissection. Postoperative histological examination confirmed a second invasive lung adenocarcinoma, measuring 0.6 cm in greatest dimension. The histological subtypes were acinar (40%) and papillary (40%), with micropapillary (20%) component. The histological grade was G3 (poorly differentiated). Immunohistochemical examination showed: Napsin A (positive); TTF-1 (SPT24) (strongly positive, ++); Ki-67 proliferation index approximately 5%. All resected lymph nodes were negative for metastasis. The pathological stage was pT1aN0cM0 (AJCC 9th edition, Stage IA1).

Genetic testing of the second tumor specimen using next-generation sequencing (NGS) revealed an EGFR T790M mutation in exon 20 and an L858R mutation in exon 21. Given the presence of the de novo T790M mutation (without prior EGFR-TKI treatment), the possibility of a germline EGFR T790M mutation was considered, and genetic counseling was recommended.

Following the second surgery, the patient was started on adjuvant almonertinib mesylate (Ameile) 110 mg (two 55 mg tablets) orally once daily, based on the presence of the EGFR T790M and L858R double mutation. The patient tolerated the medication well, without significant adverse events. At the most recent follow-up, 20 months after initiation of almonertinib therapy, the patient remained recurrence-free with no evidence of disease on chest CT.

Written informed consent for publication of this case report and accompanying images was obtained from the patient.

Discussion and Conclusions

This case report presents a patient with lung adenocarcinoma with STAS who developed a contralateral metachronous pulmonary lesion 18 months after initial lobectomy. The case highlights several important clinical issues: (1) the value of peritumoral satellite nodules on CT as a reliable preoperative indicator of STAS; (2) the utility of cinematic rendering for 3D visualization of STAS-related satellite nodules; (3) the diagnostic challenge of differentiating metachronous second primary lung cancer from pulmonary

metastasis; (4) the clinical implications of de novo EGFR T790M/L858R double mutation; and (5) the role of third-generation EGFR-TKIs in the adjuvant setting.

STAS is a recently recognized pattern of invasion in lung adenocarcinoma that has garnered significant attention since its inclusion in the 2015 WHO classification [3]. The pathogenesis of STAS remains incompletely understood. Three-dimensional histologic and immunohistochemical analyses by Yagi et al. revealed that STAS tumor cell clusters are focally attached to the alveolar walls rather than freely floating in air spaces, suggesting a mechanism of detachment from the main tumor, migration through air spaces, and reattachment to the alveolar walls through vessel co-option [6]. This mechanism may explain the higher recurrence rate observed in patients with STAS-positive tumors who undergo limited resection, as residual STAS cells in the preserved lung parenchyma may serve as a source of local recurrence [6, 7].

The prognostic significance of STAS has been extensively studied. Warth et al. demonstrated that STAS is significantly associated with male sex, lymph node and distant metastasis, advanced tumor stage, and high-grade histological patterns in a series of 569 adenocarcinomas [5]. Kadota et al. found that STAS-positive patients had a 5-year cumulative incidence of recurrence (CIR) of 42.6%, significantly higher than the 10.9% CIR in STAS-negative patients, and that STAS was an independent risk factor for recurrence after limited resection [7]. A recent study by Chen et al. confirmed that STAS is an independent risk factor for overall survival in patients with ≤ 2 cm stage IA lung adenocarcinoma [9]. Importantly, Shiono et al. demonstrated that STAS is a significant risk factor for pulmonary metastasis after surgery, with 5-year recurrence-free rates of 65.4% among STAS-positive patients versus 89.0% among STAS-negative patients [20]. In our case, the primary tumor exhibited micropapillary and poorly differentiated components—features known to be associated with STAS and aggressive tumor behavior—and the patient subsequently developed a contralateral pulmonary lesion, consistent with the known association between STAS and pulmonary recurrence.

The strong association between STAS and poor prognosis has significant implications for surgical management. A systematic review and meta-analysis by Xu et al. pooling 26 studies (12,266 patients) confirmed that lobectomy provided additional survival benefits to STAS-positive patients compared with sublobar resection [10]. Furthermore, the 2024 Chinese Medical Association guideline for lung cancer added STAS as a high-risk factor supporting postoperative adjuvant therapy in stage IB patients [18]. In the present case, lobectomy was chosen based on the preoperative imaging suspicion of STAS, and the pathological confirmation of STAS validated this surgical decision.

The development of a contralateral pulmonary lesion 18 months after initial surgery raised the critical diagnostic question of whether this represented a metastasis of the primary tumor or a metachronous second primary lung cancer (mMPLC). The differentiation between MPLC and intrapulmonary metastasis (IPM) is essential, as it determines tumor staging and treatment planning [22, 23]. The Martini-Melamed criteria, established in 1975, define mMPLC as a second tumor of the same histological type occurring at least 2 years after the primary tumor, located in a different lobe or

contralateral lung, without involvement of common lymphatic drainage pathways or extrapulmonary metastasis [22]. In our case, the 18-month interval is shorter than the 2-year disease-free interval proposed by the Martini-Melamed criteria, making the distinction between mMPLC and IPM challenging based on clinical criteria alone.

Comprehensive histologic assessment (CHA), as proposed by Girard et al., provides a valuable tool for differentiating MPLC from IPM by evaluating the percentage of histological subtypes and cytological/stromal characteristics [23]. In our case, the first tumor was acinar predominant (with 20% papillary, 15% micropapillary, and 5% poorly differentiated components), while the second tumor showed a different histological composition (40% acinar, 40% papillary, 20% micropapillary, grade 3). The different proportions of histological subtypes and the higher histological grade in the second tumor support the possibility of a second primary rather than a metastasis. However, molecular comparison between the two tumors—which would provide definitive evidence—was not available, as genetic testing was only performed on the second tumor specimen. The detection of a de novo EGFR T790M/L858R double mutation in the second tumor, in the absence of prior EGFR-TKI treatment, raises important considerations.

De novo EGFR T790M mutations, detected before any TKI treatment, are rare, occurring in less than 1% of all lung cancers and approximately 2% of EGFR-mutant lung cancers [25, 26]. Approximately 50% of de novo T790M mutations are of germline origin, and germline T790M carriers have a concomitant somatic EGFR-activating mutation (most commonly L858R) in approximately 73% of cases [25, 26, 27]. Germline EGFR T790M mutations are predominantly found in female, never-smoker patients of European descent, and are often associated with multiple bilateral ground-glass pulmonary nodules [26, 27]. The risk of developing lung cancer for germline T790M carriers is estimated to exceed 50% before age 60 [27]. In our case, the patient was a female never-smoker who developed metachronous bilateral lung adenocarcinomas, features consistent with the possibility of a germline EGFR T790M mutation. However, as genetic testing was performed only on the second tumor specimen and germline testing (using peripheral blood mononuclear cells) was not performed, we cannot definitively confirm whether the T790M mutation was somatic or germline. We strongly recommend germline testing for this patient, as a germline T790M finding would have important implications for family screening and genetic counseling [25, 27].

The relationship between STAS and EGFR mutation status has been explored in the literature. Lee et al. found that STAS was significantly associated with wild-type EGFR and that STAS was more frequently found in tumors without EGFR mutations [21]. However, STAS can also occur in EGFR-mutant tumors, and the prognostic implications of STAS may differ depending on the molecular profile [21]. In our case, molecular testing was not performed on the first (STAS-positive) tumor, precluding a direct comparison. The presence of EGFR mutations in the second tumor, particularly the de novo T790M mutation, adds a layer of complexity to the molecular characterization of this case.

The treatment approach for this patient reflects the evolving landscape of EGFR-mutant lung cancer management. Following the second surgery, adjuvant almonertinib was initiated based on the presence of the EGFR T790M/L858R double mutation. Almonertinib (aumolertinib, HS-10296) is a third-generation EGFR-TKI with potent activity against both sensitizing EGFR mutations (including L858R) and the T790M resistance mutation, with IC50 values of 0.29 nM for T790M/L858R [28]. In the phase III AENEAS trial, almonertinib significantly prolonged median progression-free survival to 19.3 months compared with 9.9 months for gefitinib in treatment-naive advanced EGFR-mutant NSCLC [29]. While osimertinib has been approved for adjuvant therapy in resected EGFR-mutant NSCLC based on the ADAURA trial, the role of almonertinib in the adjuvant setting is being investigated in ongoing clinical trials, including a phase III study comparing almonertinib versus placebo as adjuvant therapy for resected stage II-IIIB NSCLC with EGFR-sensitive mutations (NCT04687241) [30]. Our case provides real-world experience of adjuvant almonertinib use in a patient with resected EGFR T790M/L858R-mutant lung adenocarcinoma, with favorable short-term outcomes (20 months recurrence-free).

Cinematic rendering, as demonstrated in this case, offers several advantages over conventional CT reconstruction techniques for the evaluation of STAS. Unlike traditional volume rendering, cinematic rendering employs a global lighting model that simulates the physical propagation of light from thousands of virtual light sources, producing photorealistic images with enhanced depth perception, shadow rendering, and anatomical detail [14, 15]. The technique enables clear visualization of small satellite nodules surrounding the main tumor, which may be difficult to appreciate on conventional axial CT slices, and different color templates can be applied to highlight different anatomical structures, facilitating a comprehensive assessment of the tumor's relationship with adjacent structures [14, 15, 16].

Several limitations of this case report should be acknowledged. First, molecular testing was not performed on the first (STAS-positive) tumor, precluding a definitive molecular comparison between the two tumors and limiting our ability to definitively differentiate between mMPLC and IPM. Second, germline testing for EGFR T790M was not performed, and the question of whether the T790M mutation is of somatic or germline origin remains unresolved. Third, this is a single-case report, which limits the generalizability of our findings. Fourth, the follow-up period of 20 months after the second surgery is relatively short, and longer follow-up is needed to assess the long-term efficacy of adjuvant almonertinib in this setting.

In conclusion, this case report demonstrates that peritumoral satellite nodules on CT are a highly reliable indicator of STAS in lung adenocarcinoma, and that STAS-positive patients require vigilant long-term surveillance for metachronous pulmonary lesions. Cinematic rendering provides unparalleled and intuitive visualization of STAS-related satellite nodules, which may aid in preoperative STAS prediction and surgical decision-making. The finding of a de novo EGFR T790M/L858R double mutation in the metachronous lesion highlights the importance of comprehensive molecular profiling of metachronous tumors and the consideration of germline testing when de novo T790M is identified. Adjuvant almonertinib shows promising short-term results in this patient, supporting the need for further clinical trials to evaluate third-generation EGFR-TKIs in the adjuvant setting for EGFR-mutant resected lung

cancer. Precise preoperative prediction of STAS, vigilant postoperative surveillance, and individualized molecular-guided therapy are pivotal for optimizing outcomes in lung adenocarcinoma patients.

Abbreviations

STAS Spread through air spaces

WHO World Health Organization

NSCLC Non-small cell lung cancer

CT Computed tomography

3D Three-dimensional

CTR Consolidation-to-tumor ratio

CEA Carcinoembryonic antigen

CYFRA21-1 Cytokeratin-19 fragment

SCC Squamous cell carcinoma antigen

VATS Video-assisted thoracoscopic surgery

RFS Recurrence-free survival

OS Overall survival

HR Hazard ratio

CIR Cumulative incidence of recurrence

TTF-1 Thyroid transcription factor-1

EGFR Epidermal growth factor receptor

TKI Tyrosine kinase inhibitor

AJCC American Joint Committee on Cancer

MPLC Multiple primary lung cancer

sMPLC Synchronous multiple primary lung cancer

mMPLC Metachronous multiple primary lung cancer

IPM Intrapulmonary metastasis

CHA Comprehensive histologic assessment

NGS Next-generation sequencing

PD-L1 Programmed death-ligand 1

IHC Immunohistochemistry

GGO Ground-glass opacity

Declarations

Ethics approval and consent to participate

This study was conducted in accordance with the Declaration of Helsinki and was approved by the Ethics Committee of the Second Affiliated Hospital, Zhejiang University School of Medicine. The requirement for informed consent from the patient was waived due to the retrospective nature of this case report.

Consent for publication

Written informed consent for publication of this case report and accompanying images was obtained from the patient. A copy of the consent form is available for review by the Editor-in-Chief of this journal.

Competing interests

The authors declare that they have no competing interests.

Funding

Not applicable.

Author Contribution

LG analyzed and interpreted the patient imaging data and was a major contributor in writing the manuscript. BL conceived the study, interpreted the patient data, performed the cinematic rendering reconstruction, and critically revised the manuscript. All authors read and approved the final manuscript.

Acknowledgement

The authors thank the Department of Pathology, the Second Affiliated Hospital, Zhejiang University School of Medicine, for providing pathological diagnostic support.

Availability of data and materials

All data generated or analysed during this study are included in this published article and its supplementary information files. Further datasets used and/or analysed during the current study are available from the corresponding author on reasonable request.

References

1. Leiter A, Veluswamy RR, Wisnivesky JP. The global burden of lung cancer: current status and future trends. Nat Rev Clin Oncol. 2023;20(9):624–39.
2. Chen Z, Wu X, Fang T, Ge Z, Liu J, Wu Q, et al. Prognostic impact of tumor spread through air spaces for T2aN0 stage IB non-small cell lung cancer. Cancer Med. 2023;12(14):15246–55.
3. Travis WD, Brambilla E, Nicholson AG, Yatabe Y, Austin JHM, Beasley MB, et al. The 2015 World Health Organization classification of lung tumors: impact of genetic, clinical and radiologic advances since the 2004 classification. J Thorac Oncol. 2015;10(9):1243–60.
4. Nicholson AG, Tsao MS, Beasley MB, Borczuk AC, Brambilla E, Cooper WA, et al. The 2021 WHO classification of lung tumors: impact of advances since 2015. J Thorac Oncol. 2022;17(3):362–87.
5. Warth A, Muley T, Kossakowski CA, Goeppert B, Schirmacher P, Dienemann H, et al. Prognostic impact of intra-alveolar tumor spread in pulmonary adenocarcinoma. Am J Surg Pathol. 2015;39(6):793–801.
6. Yagi Y, Aly RG, Tabata K, Barlas A, Rekhtman N, Eguchi T, et al. Three-dimensional histologic, immunohistochemical, and multiplex immunofluorescence analyses of dynamic vessel co-option of spread through air spaces in lung adenocarcinoma. J Thorac Oncol. 2020;15(4):589–600.
7. Kadota K, Nitadori J, Sima CS, Ujiie H, Rizk NP, Jones DR, et al. Tumor spread through air spaces is an important pattern of invasion and impacts the frequency and location of recurrences after limited resection for small stage I lung adenocarcinomas. J Thorac Oncol. 2015;10(5):806–14.
8. Toki MI, Harrington K, Syrigos KN. The role of spread through air spaces (STAS) in lung adenocarcinoma prognosis and therapeutic decision making. Lung Cancer. 2020;146:127–33.
9. Chen X, Zhou H, Wu M, Xu M, Li T, Wang J, et al. Prognostic impact of spread through air spaces in patients with ≤ 2 cm stage IA lung adenocarcinoma. J Thorac Dis. 2024;16(4):2432–42.
10. Xu Y, Chen D, Xu X, Zhang Y, Duan S, Chen Y, et al. Impact of tumor spread through air spaces on surgical decision-making and accuracy of identifying spread through air spaces on frozen sections: a systematic review and meta-analysis. Chin J Clin Thorac Cardiovasc Surg. 2024;31(6):900–9.
11. Toyokawa G, Yamada Y, Tagawa T, Kamitani T, Yamasaki Y, Shimokawa M, et al. Computed tomography features of resected lung adenocarcinomas with spread through air spaces. J Thorac

Cardiovasc Surg. 2018;156(4):1670–6.
12. Li H, Li L, Liu Y, Deng Y, Zhu Y, Huang L, et al. Predictive value of CT and 18F-FDG PET/CT features on spread through air space in lung adenocarcinoma. BMC Cancer. 2024;24:434.
13. Peng X, Zhao H, Wu S, Jia D, Hu M, Guo B, et al. Habitat-based CT radiomics enhances the ability to predict spread through air spaces in stage T1 invasive lung adenocarcinoma. Front Oncol. 2024;14:1436189.
14. Eid M, De Cecco CN, Nance JW Jr, Caruso D, Albrecht MH, Spandorfer AJ, et al. Cinematic rendering in CT: a novel, lifelike 3D visualization technique. AJR Am J Roentgenol. 2017;209(2):370–9.
15. Brookmeyer C, Chu LC, Rowe SP, Fishman EK. Clinical implementation of cinematic rendering. Curr Probl Diagn Radiol. 2024;53(3):313–28.
16. Recht HS, Weisberg EM, Fishman EK. 3D CT cinematic rendering of pediatric thoracic vascular anomalies. Eur J Radiol Open. 2023;10:100485.
17. Lu S, Tan KS, Kadota K, Eguchi T, Bains S, Navarro-Ramirez R, et al. Spread through air spaces (STAS) is an independent predictor of recurrence and lung cancer-specific death in squamous cell carcinoma. J Thorac Oncol. 2017;12(2):223–34.
18. Chinese Medical Association. Chinese medical association guideline for clinical diagnosis and treatment of lung cancer (2024 edition). Chin J Tuberc Respir Dis. 2024;47(9):1–35.
19. Pan H, Zhao Y, Wu S, et al. Threshold of adequate resection margin for sub-lobar resection in peripheral clinical stage IA1-2 non-small cell lung cancer with tumor spread through air spaces. Lung Cancer. 2025;210:108838.
20. Shiono S, Endo M, Suzuki K, Hayasaka K, Yanagawa N. Spread through air spaces in lung cancer patients is a risk factor for pulmonary metastasis after surgery. J Thorac Dis. 2018;10(11):6469–74.
21. Lee JS, Kim EK, Kim M, Shim HS. Genetic and clinicopathologic characteristics of lung adenocarcinoma with tumor spread through air spaces. Lung Cancer. 2018;123:121–6.
22. Martini N, Melamed MR. Multiple primary lung cancers. J Thorac Cardiovasc Surg. 1975;70(4):606–12.
23. Girard N, Deshpande C, Lau C, Finley D, Rusch V, Pao W, et al. Comprehensive histologic assessment helps to differentiate multiple lung primary nonsmall cell carcinomas from metastases. Am J Surg Pathol. 2009;33(12):1752–64.
24. Costa AS Jr, Gellada N. Cinematic rendering for three-dimensional reconstructions of the chest wall: a new reality. Einstein (São Paulo). 2020;18:eMD5223.
25. Oxnard GR, Lo PC, Nishino M, Dahlberg SE, Lindeman NI, Butaney M, et al. Lifetime risk of lung cancer in germline EGFR T790M carriers. J Clin Oncol. 2017;35(15suppl):8580.
26. Bell DW, Gore I, Okimoto RA, Godin-Heymann N, Sordella R, Mulloy R, et al. Inherited susceptibility to lung cancer may be associated with the T790M drug resistance mutation in EGFR. Nat Genet. 2005;37(12):1315–16.

27. Gazdar A, Robinson L, Oliver D, Xing C, Travis WD, Soh J, et al. Hereditary lung cancer syndrome targets never smokers with germline EGFR T790M mutations. J Thorac Oncol. 2014;9(4):456–63.
28. Yang JC, Camidge DR, Yang CT, Zhou J, Yan Y, Hu J, et al. Safety, efficacy, and pharmacokinetics of almonertinib (HS-10296) in pretreated patients with EGFR-mutated advanced NSCLC: a multicenter, open-label, phase 1 trial. J Thorac Oncol. 2020;15(12):1907–18.
29. Lu S, Dong X, Jian H, Li L, Chen L, Xu H, et al. AENEAS: a randomized phase III trial of aumolertinib versus gefitinib as first-line therapy for locally advanced or metastatic EGFR-mutated non-small-cell lung cancer. J Clin Oncol. 2022;40(27):3162–71.
30. Lu S, Wang Q, Zhang G, Dong X, Yang CT, Song Y, et al. Efficacy of aumolertinib (HS-10296) in patients with advanced EGFR T790M+ NSCLC: updated post-National Medical Products Administration approval results from the APOLLO registrational trial. J Thorac Oncol. 2022;17(3):411–22.
31. Jia M, Yu S, Gao H, Sun PL. Spread through air spaces (STAS) in lung cancer: a multiple-perspective and update review. Cancer Manag Res. 2020;12:2743–52.
32. Onozato ML, Kovach AE, Yeap BY, Morales-Oyarvide V, Klepeis VE, Taff TS, et al. Tumor islands in resected early-stage lung adenocarcinomas are associated with unique clinicopathologic molecular characteristics and worse prognosis. Am J Surg Pathol. 2013;37(2):287–94.

Figures



Figure 1

Chest CT and cinematic rendering findings of the primary tumor in the left lower lobe. (A) Axial chest CT shows a mass lesion in the superior segment of the left lower lobe with multiple satellite nodules (arrow). (B) Coronal chest CT demonstrates the mass lesion with surrounding satellite nodules (arrow). (C and D) Images postprocessed using cinematic rendering with different color templates clearly show metastatic small solid nodules surrounding the lesion. (E and F) Images using cinematic rendering

clearly show the relationship of the lesion with the bronchus and lung parenchyma. The cinematic rendering technique provides superior depth perception and 3D visualization of the satellite nodules and their spatial relationship with adjacent anatomical structures compared with conventional CT images.

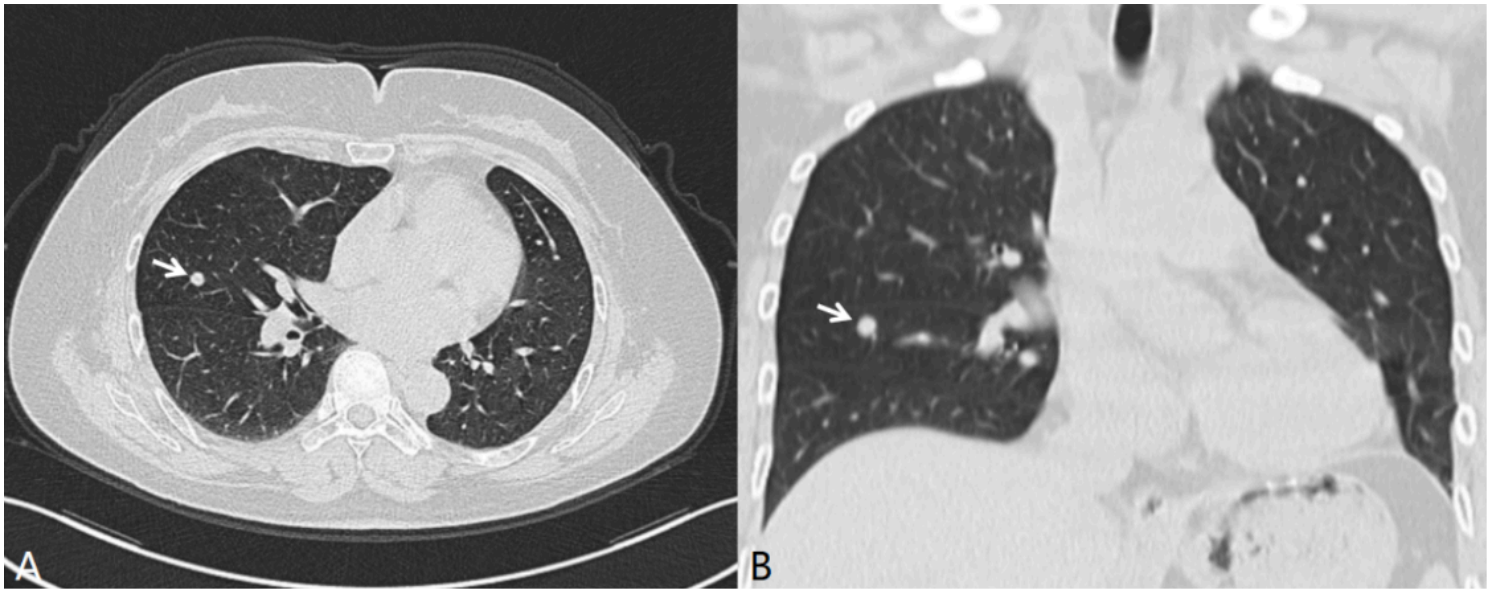


Figure 2

Follow-up chest CT 18 months after the first surgery showing a new nodule in the right middle lobe. (A) Axial chest CT reveals a new solid nodule measuring 0.6 cm in the right middle lobe (arrow). (B) Coronal chest CT demonstrates the nodule in the right middle lobe (arrow). Pathological examination after resection confirmed a second invasive lung adenocarcinoma with EGFR T790M/L858R double mutation.